

Current Opinion in Chemical Biology – invited Review article (November 2016)

Diversity of Fe²⁺ entry and oxidation in ferritins

Justin M. Bradley, Geoffrey R. Moore and Nick E Le Brun¹

Centre for Molecular and Structural Biochemistry, School of Chemistry, University of East Anglia, Norwich NR4 7TJ, UK

¹Address correspondence to: Nick E Le Brun, School of Chemistry, University of East Anglia, Norwich NR4 7TJ, UK. Tel. +44 1603 592699; Fax. +44 1603 592003; Email: n.le-brun@uea.ac.uk

Abstract

The essential metal iron presents two major problems for life: it is potentially highly toxic due to its redox activity, and its extremely low solubility in aqueous solution in the presence of O₂ can make it hard to acquire and store safely. Ferritins are part of nature's answer to these problems, as they store iron in a safe but accessible form in all types of cells. How they achieve this has been the subject of intense research for several decades. Here, we highlight recent progress in elucidating the routes by which Fe²⁺ ions access the catalytic ferroxidase centers, and the mechanisms by which Fe²⁺ is oxidized. Emerging from this is a picture of diversity, both in terms of Fe²⁺ entry pathways and the roles played by the structurally distinct diiron ferroxidase centers.

Introduction

Iron is essential for virtually all of life. Its ability to redox-cycle at physiologically relevant reduction potentials underpins many of its functions, but also makes it potentially toxic to aerobically respiring cells. In addition, the most stable oxidation state of iron in the presence of molecular oxygen is Fe^{3+} , which is only vanishingly soluble. Thus, despite being the fourth most abundant element of the earth's crust, iron is poorly available to the majority of life, and is often a limiting nutrient. To overcome the challenges associated with iron, sophisticated mechanisms of iron sequestration and detoxification have evolved and central to these are the ferritins, a family of proteins that function as iron stores and/or detoxifiers in all Kingdoms of life [1,2].

Ferritins are composed of 24 α -helical subunits that assemble to form a rhombic dodecahedral protein shell (overall 4 3 2 symmetry) with a pair of subunits at each of the twelve faces, see Figure 1a. Channels, located at the six four-fold and eight three-fold axes, connect the exterior of the protein with the central cavity, which is approx. 80 Å in diameter. Large amounts of iron, in the form of a hydrous ferric oxy-hydroxide mineral of variable crystallinity, can be reversibly stored in the cavity. Animal ferritins are generally composed of two types of subunit, H-chain and L-chain. These share significant amino acid residue identity (~55% overall and ~80% for residues at the subunit interface) and are isostructural such that different proportions of H- and L-chain subunits can assemble to form essentially the same three dimensional structure, as found in ferritins from different tissues [3]. A major difference between the subunits is that the H-chain contains a catalytic diiron site located at the center of the four α -helical bundle of the subunit (Figure 1b). This catalytic site, called the ferroxidase center, drives the formation of the iron mineral through the oxidation of Fe^{2+} to Fe^{3+} .

Plant ferritins also form heteropolymers in at least some cases but here both subunits are of the H-chain variety. Prokaryotic ferritins are of two principal types: bacterioferritins (BFRs) only isolated from bacteria and the non-heme prokaryotic ferritins (Ftns), also found in archaea [4]. Prokaryotic ferritins appear to be homopolymers of subunits containing a ferroxidase center and are therefore referred to as H-chain type, but overall they have relatively low (~20%) sequence identity to eukaryotic H-chain ferritins. The structure of the ferroxidase centre differs between Ftns and BFRs and both are distinct from that of eukaryotic H-chains, see Figure 1b - d).

In this review, we survey the recent literature on various aspects of the mineralization process, including Fe^{2+} uptake pathways, Fe^{2+} oxidation, the fate of the resulting Fe^{3+} and the roles of protein radicals. Together, these reveal major structural and mechanistic variation within the ferritin family.

Fe^{2+} accesses the ferroxidase centers of vertebrate ferritins via three-fold channels

To initiate mineralization, Fe^{2+} must be able to access the ferroxidase centers and internal cavity. How this occurs has recently become clearer. A large body of work, mainly from the Theil and Turano groups, has established the importance of the 15 Å-long, hydrophilic three fold channels for access of Fe^{2+} to the ferroxidase centers. Initial structural information was obtained for frog M ferritin crystals using Co^{2+} and Mg^{2+} as probes for labile Fe^{2+} sites [5]. This, together with dramatic effects on ferroxidase center activity observed for site-directed channel variants, revealed a pathway for Fe^{2+} from the protein exterior, through the three fold channels towards the ferroxidase sites. Channel residues Asp127 and Glu130 together with residues Glu136 and Glu57, located within the subunit helical bundle, were shown to be important for guiding Fe^{2+} from the three fold channels into the ferroxidase center [6-8].

More recently, high-resolution structures of iron bound within the three-fold channels of frog ferritin have been reported. Two fully hydrated Fe^{2+} ($[\text{Fe}(\text{H}_2\text{O})_6]^{2+}$) ions were observed, hydrogen bonded to Asp127 and Glu130 [9]. This was surprising because fully hydrated Fe^{2+} ion has a diameter of 6.9 Å and was previously thought to be too large to traverse the channel without partial/full dehydration or channel conformational flexing/channel widening [10]. However, the new structural data are clear and supported by molecular dynamics simulations of the channel containing two hexaaqua Fe^{2+} ions [11]. This is the first structural evidence of the transit of $[\text{Fe}(\text{H}_2\text{O})_6]^{2+}$ ions through ferritin three-fold channels. Parallel studies

of human H-chain ferritin (HuHF) revealed the same two $[\text{Fe}(\text{H}_2\text{O})_6]^{2+}$ ions coordinated by Asp131 and Glu134 in the three-fold channels, see Figure 2a and b.

Time-resolved crystallographic analysis of frog M-chain ferritin utilising a novel method of crystal soaking involving exposure to crystalline Fe^{2+} salt in the presence of catalytically inhibitory concentrations of Mg^{2+} enabled direct observation of transient Fe^{2+} -binding sites close to the ferroxidase center (Figure 2c) [9]. Amongst the three sites, Fe3 (coordinated by His54, Glu57, Glu103 and Asp140) and Fe4 (coordinated by Glu57, Glu136 and Asp140), were observed in both anaerobically and aerobically soaked crystals (though the coordination of Fe3 was less well defined under aerobic conditions) and closely align with Co^{2+} sites observed when this metal was used as a proxy for Fe^{2+} -binding [5]. Fe2/Fe3 and Fe3/Fe4 sites are sufficiently close to one another to preclude simultaneous occupancy, consistent with Fe3 and Fe4 representing transient binding sites for Fe^{2+} ions as they move into the ferroxidase center. Observed occupancies are also consistent with this, with longer aerobic exposure times revealing Fe^{2+} bound only at sites Fe1 and Fe2.

Similar time-resolved studies have also been reported for HuHF [12]. The two proteins share 64% identity including all iron-coordinating residues at the ferroxidase center. However, X-ray structures of iron-soaked crystals revealed differences in the transit sites from the channels into the ferroxidase centers. Four sites, Fe1-Fe4, were observed but sites 3 and 4 are not conserved between the two proteins. Gln58 replaces His54 of frog M as a ligand to Fe3 in HuHF and Fe4 is coordinated only by Glu61, His57 and four water molecules as opposed to the three carboxylate residues in frog M-ferritin (Figure 2d). In further contrast to frog M-ferritin, the occupancy of the four sites did not vary at aerobic Fe^{2+} soaking times greater than 5 min. The Fe1 site exhibited the highest occupancy at ~70% after 1 min and ~100% after 5 min (and onwards). Fe2-4 occupancy ranged from 20-50% as exposure time increased and these did not decrease as was observed for frog ferritin.

These data elucidate a pathway for the transfer of Fe^{2+} into vertebrate H-chain ferritin, starting with binding of hydrated Fe^{2+} in the three-fold channels, followed by stepwise desolvation and binding at sites close to the ferroxidase center, which vary in nature between vertebrate ferritins, before reaching ferroxidase sites Fe1 and Fe2. The occupancies are entirely consistent with previous data [13-15] in that they indicate that Fe1 is the higher affinity site for metal ions in vertebrate ferritins.

Fe^{2+} accesses the ferroxidase centers of BFRs via B-channels

Much less is known about the routes for Fe^{2+} entry into the ferroxidase centers of prokaryotic ferritins. The similarity of the three-fold channels to those of animal ferritins makes them attractive candidates, but attempts to disrupt them in *E. coli* BFR proved inconclusive [16]. Metal ions, including iron, have been observed at four-fold channels of some ferritins suggesting that these might serve as entry routes [17] and a short route from the surface directly to the ferroxidase center was recently proposed for Ftn proteins [18]. Prokaryotic ferritins contain an additional 24 channels, so called B-channels, which occur at the edges of each face of the dodecahedron where one subunit dimer meets another side on [19]. B-channels are generally lined with charged or hydrophilic residues, and thus represent another possible route for iron to enter the protein and metal ions have been observed bound in the channels in some BFR structures [17,20]. Substitution of *E. coli* BFR B-channel residue Asp132 by Phe resulted in a significant decrease in not only the rate of mineralization, but also in the rate of the initial ferroxidase center reaction [21]. Structural data showed that the substitution caused a steric blockage of the B-channel with no other material structural perturbation (Figure 2e). An acidic inner surface patch that connects the B-channel to the ferroxidase center (a distance of ~22 Å) suggests a route that Fe^{2+} might take and we note that replacement of Glu47, which forms part of the patch, with Asn significantly lowered the rate of initial Fe^{2+} oxidation at the ferroxidase center [22]. These data demonstrate that the B-channels are a major route for iron entry into both the ferroxidase center and the iron storage cavity of BFR.

While B-channels are absent from animal ferritins, they are present in the ferritin from the diatom *P. multiseriis*, consistent with its Ftn-like ferroxidase center. Soaking crystals of

an E44Q variant of this ferritin in an Fe^{2+} solution overnight led to iron binding in some of the B-channels, close to the inner surface coordinated by Glu35, Asp30 and two water molecules (Figure 2f) [23].

Mechanisms of Fe^{2+} oxidation and O_2 reduction

For vertebrate ferritins, reaction of the two Fe^{2+} ions at the ferroxidase center with O_2 results in their oxidation and reduction of O_2 to hydrogen peroxide, yielding an iron to O_2 ratio of 2:1 [24,25]. The reaction proceeds via a blue diferric peroxo (DFP) intermediate [26,27] ultimately generating an unstable μ -1,2-oxodiferric species. Fe^{3+} species migrate to the central cavity to become part of the mineral core. Labile Fe^{3+} at the ferroxidase center is consistent with difficulties over many years to obtain high-resolution structures of iron-bound forms of the H-chain ferroxidase center. Although this has recently been achieved the occupancies observed, particularly for site Fe2, are consistent with instability of the oxidized form of the center [9,12,26,27]. NMR experiments, in which the relaxation effects of paramagnetic Fe^{3+} on resonances of specific residues were detected, indicated that Fe^{3+} takes a route along the long axis of the subunit, emerging at the four-fold axis where it enters the cavity [28]. The high symmetry of this site might favor the nucleation of nascent iron minerals as soon as they exit the subunit. A summary of the mechanism is shown in Figure 3a.

Mineralization in Ftn proteins occurs via a mechanism related to that of H-chain ferritins but is complicated by the presence of site C. A blue colored intermediate has been observed for *E. coli* FtnA and *P. furiosus* Ftn [29-32], and structural evidence for a peroxy-diFe(III) species similar to that of vertebrate ferritins was recently reported [18]. The intermediate decays to give a μ -oxo-bridged Fe^{3+} dimer, which is apparently significantly more stable than its vertebrate ferritin counterpart, such that Fe^{3+} bound forms of the ferroxidase center of Ftn proteins are readily obtained. The role of site C appears to vary in different Ftn proteins (Figure 3b and c). In some, site C-bound Fe^{2+} participates in ferroxidase center Fe^{2+} oxidation, resulting in a higher Fe: O_2 ratio. An *E. coli* FtnA variant lacking site C exhibited only a small decrease in oxidation rate, but the Fe^{2+} : O_2 ratio dropped from 3-4 to 2 [29,30] and a more rapid regeneration of the initial rapid oxidation phase was observed, leading to behavior similar to vertebrate H-chain ferritins. Hence the site was proposed to be important for controlling iron flux through the ferroxidase center [29]. In contrast, loss of site C from *P. furiosus* Ftn led to a dramatic reduction in the initial Fe^{2+} oxidation rate, indicating that ferroxidase center activity in this Ftn is dependent on site C [33]. In other Ftn proteins, site C has no redox function but instead functions principally to limit iron flux through the ferroxidase center. *P. multiseriens* Ftn exhibits an extremely rapid ferroxidase center reaction (amongst the fastest reported) but mineralizes extremely slowly [34]. Substitution of the site C ligand Glu130 with Ala resulted in a 10 fold increase in mineralization activity whilst ferroxidase center function was unaffected [23]. This led to the proposal that the protein may function to buffer iron availability by rapidly scavenging and holding it at the ferroxidase center, facilitating iron-sparing over long-term iron storage [23].

Even within the BFRs there is significant mechanistic variation. *Pseudomonas aeruginosa* BFR is similar to vertebrate H-chain ferritins in that its ferroxidase center functions as an iron pore [35]. In contrast, that of *E. coli* BFR functions as a true catalytic center, continually cycling between its oxidized (bridged di- Fe^{3+}) and reduced (di- Fe^{2+}) forms to drive oxidation of Fe^{2+} ions in the central cavity (Figure 3d). This is reflected by the stability of the center in both Fe^{2+} and Fe^{3+} states, as demonstrated by spectroscopy and crystallography [16,36,37].

Such a mechanism requires an electron transfer pathway between the cavity and the ferroxidase center, and a key player in this is an inner surface Fe^{2+} -binding site located ~ 10 Å away from the ferroxidase center coordinated by His46, Asp50 and three water molecules. Disruption of the site by mutagenesis did not affect the ability of the ferroxidase center to oxidise Fe^{2+} but severely inhibited subsequent mineralization [36]. More recently, other important components of the electron transfer pathway were identified. Three aromatic residues (Tyr25, Tyr58 and Trp133) were also shown to be essential for mineralization but not the initial oxidation of Fe^{2+} at the ferroxidase center [38]. Identification of Tyr25 as a site of

transient radical formation led to the proposal that the two electrons required for reduction of the di-Fe³⁺ ferroxidase center are derived from the inner surface site Fe²⁺ and Tyr25, with the radical being subsequently quenched by oxidation of a second Fe²⁺ ion in the cavity (possibly also at the inner surface site). This guarantees near simultaneous delivery of two electrons to the ferroxidase center avoiding the possibility of its single electron reduction or that of O₂. Tyr58 and Trp133 are not essential for the observation of the Tyr25 radical but recent data show that, in their absence, the radical forms and decays much more slowly (our unpublished data). Thus the ferroxidase center of BFR should not be considered simply as a diiron site, but rather as a diiron site surrounded by a network of aromatic residues that facilitate its function.

As a class II diiron protein, the BFR ferroxidase center is very similar to that of other examples of such proteins including the R2 subunit of ribonucleotide reductase (RNR). The similarity with RNR is even more striking given that a functionally essential stable radical is formed on Tyr122 close to the diiron center [39]. Tyr25 and Trp133 of BFR are in very similar positions to Tyr122 and Trp48 of RNR, but on the other side of the diiron site, raising the intriguing possibility that properties of radical transfer away from the diiron center are shared between these proteins.

Tyr25 of BFR is strictly conserved in all H-chain type ferritins and is the site of radical formation in at least some other ferritins, including HuHF and Ftn proteins from *E. coli* and *P. furiosus* [30,33,40]. For Ftns, this led to the proposal that, in addition to the two electron reduction of O₂ generating H₂O₂, an additional, parallel mechanism operates involving the oxidation of Tyr24 (Ftn numbering) to a radical [30,33], which, along with oxidation of Fe²⁺ ions at the ferroxidase center and site C, results in reduction of O₂ to water, accounting for the variability in the Fe:O₂ ratio observed in Ftn proteins. Consistent with this, substitution of Tyr24 in *E. coli* FtnA significantly affected mineralization but not the ferroxidase site reaction [30]. However, in *P. furiosus* Ftn, Tyr24 was found to be essential for the initial oxidation of Fe²⁺ at the ferroxidase center [33], inconsistent with a parallel mechanism. The functional importance of radical formation on Tyr34 of HuHF is less clear [33,40]. In the absence of Tyr34 the rate of the initial ferroxidase center reaction was affected but the overall capacity to mineralize iron was not. As with the role of site C in Ftns, the function of the conserved Tyr appears to differ between ferritins.

Concluding remarks and future perspectives

Recent work on HuHF and *P. furiosus* Ftn has led to the proposal that ferritins function via a common 'universal' mechanism [15,31,33]. This proposal is partly based on the assertion that HuHF contains a site C. However, the justification for this is weak, and the recent structures of iron bound forms of HuHF and frog M-chain ferritin demonstrate that there is no site C in vertebrate ferritins. While there are binding sites for Fe²⁺ near to the ferroxidase centers, these are likely transient transport sites for Fe²⁺ ion *en route* to the ferroxidase center and vary between ferritins [9,12]. Furthermore, the recent reports on *E. coli* BFR and diatom ferritin [23,38] clearly demonstrate that ferritins, whilst sharing broadly similar structural and functional properties, exhibit significant diversity such that no single mineralization mechanism can account for all observations. Diversity amongst ferritins extends to the routes of Fe²⁺ entry into the central cavity [12,21]. Remaining challenges in understanding mineralization are in extending the excellent recent work in defining the various pathways of iron entry into and exit from the ferroxidase center, and in better understanding of the function of the conserved Tyr residue, which at least in some ferritins, supports radical formation.

Acknowledgements

Our work on ferritins has been supported by the Biotechnology and Biological Sciences Research Council UK, most recently through grant BB/I021884/1 and the Leverhulme Trust (Emeritus Fellowship to GRM, EM-2014-088). We thank Prof. Grant Mauk and Prof. Michael Murphy (Univ. of British Columbia), and Dr Dima Svistunenko (Univ. of Essex) for fruitful recent collaborations.

References

1. Bradley JM, Le Brun NE, Moore GR: **Ferritins: furnishing proteins with iron.** *J Biol Inorg Chem* 2016, **21**:13-28.
2. Theil EC, Behera RK, Tosha T: **Ferritins for Chemistry and for Life.** *Coord Chem Rev* 2013, **257**:579-586.
3. Chasteen ND, Harrison PM: **Mineralization in ferritin: An efficient means of iron storage.** *J Struct Biol* 1999, **126**:182-194.
4. Le Brun NE, Crow A, Murphy MEP, Mauk AG, Moore GR: **Iron core mineralisation in prokaryotic ferritins.** *Bioch Biophys Acta* 2010, **1800**:732-744.
5. Tosha T, Ng HL, Bhattasali O, Alber T, Theil EC: **Moving metal ions through ferritin-protein nanocages from three-fold pores to catalytic sites.** *J Am Chem Soc* 2010, **132**:14562-14569.
6. •• Behera RK, Theil EC: **Moving Fe²⁺ from ferritin ion channels to catalytic OH centers depends on conserved protein cage carboxylates.** *Proc Natl Acad Sci U S A* 2014, **111**:7925-7930.
Reports the kinetic analysis of frog M-ferritin variants, giving the first evidence for the existence of Fe²⁺ transfer sites close to the ferroxidase center.
7. Haldar S, Bevers LE, Tosha T, Theil EC: **Moving Iron through ferritin protein nanocages depends on residues throughout each four alpha-helix bundle subunit.** *J Biol Chem* 2011, **286**:25620-25627.
8. Tosha T, Behera RK, Theil EC: **Ferritin ion channel disorder inhibits Fe(II)/O₂ reactivity at distant sites.** *Inorg Chem* 2012, **51**:11406-11411.
9. •• Pozzi C, Di Pisa F, Lalli D, Rosa C, Theil E, Turano P, Mangani S: **Time-lapse anomalous X-ray diffraction shows how Fe²⁺ substrate ions move through ferritin protein nanocages to oxidoreductase sites.** *Acta Crystallogr D Biol Crystallogr* 2015, **71**:941-953.
Reports the structural analysis of frog M-ferritin, revealing sites Fe3 and Fe4 as Fe²⁺ transit sites close to the ferroxidase center, and two fully aquated Fe²⁺ ions in the three-fold channels, providing the first evidence that the hydrated ferrous ion can traverse the channel.
10. Barnes CM, Theil EC, Raymond KN: **Iron uptake in ferritin is blocked by binding of [Cr(TREN)(H₂O)(OH)]²⁺, a slow dissociating model for [Fe(H₂O)₆]²⁺.** *Proc Natl Acad Sci U S A* 2002, **99**:5195-5200.
11. Chandramouli B, Bernacchioni C, Di Maio D, Turano P, Brancato G: **Electrostatic and structural bases of Fe²⁺ Translocation through ferritin channels.** *J Biol Chem* 2016. DOI: 10.1074/jbc.M116.748046
12. •• Pozzi C, Di Pisa F, Bernacchioni C, Ciambellotti S, Turano P, Mangani S: **Iron binding to human heavy-chain ferritin.** *Acta Crystallogr D Biol Crystallogr* 2015, **71**:1909-1920.
Provides structural data for human H-chain ferritin that is consistent with that previously reported for frog ferritin, revealing transit sites close to the ferroxidase center, and two fully aquated Fe²⁺ ions in the three-fold channels. Importantly, sites Fe3 and Fe4 are different from those of frog ferritin, consistent with the lack of conserved iron sites outside of the ferroxidase center in vertebrate ferritins.
13. Hwang J, Krebs C, Huynh BH, Edmondson DE, Theil EC, Penner-Hahn JE: **A short Fe-Fe distance in peroxodiferric ferritin: Control of Fe substrate versus cofactor decay?** *Science* 2000, **287**:122-125.
14. Bou-Abdallah F, Arosio P, Santambrogio P, Yang X, Janus-Chandler C, Chasteen ND: **Ferrous ion binding to recombinant human H-chain ferritin. An isothermal titration calorimetry study.** *Biochemistry* 2002, **41**:11184-11191.
15. Ebrahimi KH, Bill E, Hagedoorn PL, Hagen WR: **The catalytic center of ferritin regulates iron storage via Fe(II)-Fe(III) displacement.** *Nat Chem Biol* 2012, **8**:941-948.

16. Le Brun NE, Andrews SC, Guest JR, Harrison PM, Moore GR, Thomson AJ: **Identification of the ferroxidase center of *Escherichia coli* bacterioferritin.** *Biochem J* 1995, **312**:385-392.
17. Swartz L, Kuchinskas M, Li HY, Poulos TL, Lanzilotta WN: **Redox-dependent structural changes in the *Azotobacter vinelandii* bacterioferritin: New insights into the ferroxidase and iron transport mechanism.** *Biochemistry* 2006, **45**:4421-4428.
18. Kim S, Lee JH, Seok JH, Park YH, Jung SW, Cho AE, Lee C, Chung MS, Kim KH: **Structural basis of novel iron-uptake route and reaction intermediates in ferritins from Gram-negative bacteria.** *J Mol Biol* 2016. <http://dx.doi.org/10.1016/j.jmb.2016.10.022>.
19. Macedo S, Romao CV, Mitchell E, Matias PM, Liu MY, Xavier AV, LeGall J, Teixeira M, Lindley P, Carrondo MA: **The nature of the di-iron site in the bacterioferritin from *Desulfovibrio desulfuricans*.** *Nat Struct Biol* 2003, **10**:285-290.
20. Janowski R, Auerbach-Nevo T, Weiss MS: **Bacterioferritin from *Mycobacterium smegmatis* contains zinc in its di-nuclear site.** *Prot Sci* 2008, **17**:1138-1150.
21. •• Wong SG, Grigg JC, Le Brun NE, Moore GR, Murphy ME, Mauk AG: **The B-type channel is a major route for iron entry into the ferroxidase center and central cavity of bacterioferritin.** *J Biol Chem* 2015, **290**:3732-3739.
Reports the kinetic and structural analysis of BFR B-channel variants, providing the first clear evidence that these channels are important routes of Fe²⁺ entry into the BFR central cavity, and that Fe²⁺ ions enter the ferroxidase center via the central cavity.
22. Wong SG, Tom-Yew SAL, Lewin A, Le Brun NE, Moore GR, Murphy MEP, Mauk AG: **Structural and mechanistic studies of a stabilized subunit dimer variant of *Escherichia coli* bacterioferritin identify residues required for core formation.** *J Biol Chem* 2009, **284**:18873-18881.
23. •• Pfaffen S, Bradley JM, Abdulqadir R, Firme MR, Moore GR, Le Brun NE, Murphy ME: **A diatom ferritin optimized for iron oxidation but not iron storage.** *J Biol Chem* 2015, **290**:28416-28427.
Reveals the function of site C in the diatom ferritin: substitution of the ligand Glu130 with Ala gave a 10-fold increase in mineralization rate, consistent with a role for site C in limiting the flux of Fe³⁺ out of the center. Also reveals Fe²⁺ binding in the B-channels of a Glu44Gln variant, providing the first evidence of iron binding in B-channels of an Ftn-type ferritin.
24. Jameson GNL, Jin W, Krebs C, Perreira AS, Tavares P, Liu XF, Theil EC, Huynh BH: **Stoichiometric production of hydrogen peroxide and parallel formation of ferric multimers through decay of the diferric- peroxo complex, the first detectable intermediate in ferritin mineralization.** *Biochemistry* 2002, **41**:13435-13443.
25. Zhao GH, Bou-Abdallah F, Arosio P, Levi S, Janus-Chandler C, Chasteen ND: **Multiple pathways for mineral core formation in mammalian apoferritin. The role of hydrogen peroxide.** *Biochemistry* 2003, **42**:3142-3150.
26. Bou-Abdallah F, Zhao GH, Mayne HR, Arosio P, Chasteen ND: **Origin of the unusual kinetics of iron deposition in human H- chain ferritin.** *J Am Chem Soc* 2005, **127**:3885-3893.
27. Pereira AS, Small W, Krebs C, Tavares P, Edmondson DE, Theil EC, Huynh BH: **Direct spectroscopic and kinetic evidence for the involvement of a peroxodiferric intermediate during the ferroxidase reaction in fast ferritin mineralization.** *Biochemistry* 1998, **37**:9871-9876.
28. •• Turano P, Lalli D, Felli IC, Theil EC, Bertini I: **NMR reveals pathway for ferric mineral precursors to the central cavity of ferritin.** *Proc Natl Acad Sci U S A* 2010, **107**:545-550.
Reports the application of advanced NMR methods to chart the pathway of Fe³⁺ ions on route from the ferroxidase center to the central cavity. Remarkably, iron traverses the long axis of the bundle, exiting at the four-fold channels. The mechanistic analysis

apart, this is a tour-de force in terms of assigning NMR signals to specific nuclei of the protein.

29. Treffry A, Zhao ZW, Quail MA, Guest JR, Harrison PM: **How the presence of three iron binding sites affects the iron storage function of the ferritin (EcFtnA) of *Escherichia coli***. *FEBS Lett* 1998, **432**:213-218.
30. • Bou-Abdallah F, Yang H, Awomolo A, Cooper B, Woodhall MR, Andrews SC, Chasteen ND: **Functionality of the three-site ferroxidase center of *Escherichia coli* bacterial ferritin (EcFtnA)**. *Biochemistry* 2014, **53**:483-495.
Reveals the existence of multiple oxidation mechanisms in FtnA and the formation of a radical species on Tyr24, the strictly conserved near-ferroxidase center residue.
31. Ebrahimi KH, Bill E, Hagedoorn PL, Hagen WR: **Spectroscopic evidence for the role of a site of the di-iron catalytic center of ferritins in tuning the kinetics of Fe(II) oxidation**. *Mol Biosyst* 2016, **12**:3576-3588.
32. Zhao ZW, Treffry A, Quail MA, Guest JR, Harrison PM: **Catalytic iron(II) oxidation in the non-haem ferritin of *Escherichia coli*: the early intermediate is not an iron tyrosinate**. *Dalton Trans* 1997:3977-3978.
33. • Ebrahimi KH, Hagedoorn PL, Hagen WR: **A conserved tyrosine in ferritin is a molecular capacitor**. *Chembiochem* 2013, **14**:1123-1133.
Reveals the importance of the strictly conserved near-ferroxidase center Tyr residue for ferroxidase center activity and formation of a Tyr radical.
34. Pfaffen S, Abdulqadir R, Le Brun NE, Murphy ME: **Mechanism of ferrous iron binding and oxidation by ferritin from a pennate diatom**. *J Biol Chem* 2013, **288**:14917-14925.
35. Weeratunga SK, Lovell S, Yao H, Battaile KP, Fischer CJ, Gee CE, Rivera M: **Structural studies of bacterioferritin B from *Pseudomonas aeruginosa* suggest a gating mechanism for iron uptake via the ferroxidase center**. *Biochemistry* 2010 **49**:1160-1175.
36. Crow A, Lawson TL, Lewin A, Moore GR, Le Brun NE: **Structural basis for iron mineralization by bacterioferritin**. *J Am Chem Soc* 2009, **131**:6808-6813.
37. •• Kwak Y, Schwartz JK, Huang VW, Boice E, Kurtz DM, Jr., Solomon EI: **CD/MCD/VTM-MCD Studies of *Escherichia coli* bacterioferritin support a binuclear iron cofactor site**. *Biochemistry* 2015, **54**:7010-7018.
Reports advanced spectroscopic studies of *E. coli* BFR, providing direct evidence of the inner surface Fe²⁺-binding site and showing conclusively that the ferroxidase center can be redox cycled without loss of iron.
38. •• Bradley JM, Svistunenko DA, Lawson TL, Hemmings AM, Moore GR, Le Brun NE: **Three aromatic residues are required for electron transfer during iron mineralization in bacterioferritin**. *Angew Chem Int Ed Engl* 2015, **54**:14763-14767.
Reveals that iron mineralization in *E. coli* BFR proceeds via a radical mechanism, involving transient formation of a radical on the strictly conserved near-ferroxidase center Tyr residue. This accounts for how the two electron re-reduction of the di-Fe³⁺ center can occur efficiently even under low iron conditions.
39. Minnihhan EC, Nocera DG, Stubbe J: **Reversible, long-range radical transfer in *E. coli* class Ia ribonucleotide reductase**. *Acc Chem Res* 2013, **46**:2524-2535.
40. Chen-Barrett Y, Harrison PM, Treffry A, Quail MA, Arosio P, Santambrogio P, Chasteen ND: **Tyrosyl radical formation during the oxidative deposition of iron in human apoferritin**. *Biochemistry* 1995, **34**:7847-7853.

Figure legends

Figure 1.

Overall structure of ferritins and the variability of their catalytic ferroxidase centers. **(a)** Ribbon diagram showing the backbone structure common to all 24mer ferritins. Each of the subunits are coloured differently and the protein is viewed down a three-fold channel (pdb 2JD7). **(b)** The H-chain ferroxidase center. Fe1 is ligated by a histidine, a monodentate glutamate and a bridging glutamate, while Fe2 is ligated by the same bridging glutamate and a terminal glutamate only (pdb 4OYN). **(c)** The ferroxidase center of Ftn. Fe-A has the same coordination as observed for Fe1 in H-chain, while Fe-B is similar to Fe2 but has additional glutamate ligand (here, Glu130). This additional glutamate ligand is actually a bridging ligand to a third iron-binding site, Fe-C (or site C), which is also coordinated by three further glutamates (pdb 2JD7). **(d)** The ferroxidase center of BFR. This center is much more symmetric than those of other ferritins: Fe-A and Fe-B are both coordinated by terminal glutamates and histidines, and by two bridging glutamates residues (pdb 3E1N). The BFR ferroxidase center is the only ferritin site that belongs to class II of the dinuclear iron site proteins.

Figure 2.

Iron transport routes in ferritins. **(a)** A view down the three fold channel of HuHF showing $[\text{Fe}(\text{H}_2\text{O})_6]^{2+}$ H-bonded to three symmetry related Glu134 residues (pdb 4OYN). **(b)** A perpendicular view of the same three-fold channel showing that another fully aquated Fe^{2+} ion is bound in the channel immediately below by Asp131 (pdb 4OYN). **(c)** and **(d)** Transit sites *en route* to the ferroxidase center of frog ferritin (pdb 4LYU) and HuHF (pdb 4ZJK), respectively. Sites Fe3 and Fe4, which are distinct in the two proteins, are shown. Note that in frog ferritin the sites cannot be simultaneously occupied. **(e)** B-channel of *E. coli* BFR. Substitution of Asp132 with Phe leads to a blocking of the channel, with the result that the initial ferroxidase center reaction and mineralization are inhibited (pdb 3E1L and 4U3G). **(f)** Fe^{2+} bound at the B-channel of diatom (*P. multiseriis*) ferritin, coordinated by Glu35, Asp30 and two water molecules (pdb 4ZKH). In (a) the mesh represents the surface of the channel carboxylates and in (e) the surface of F132. In (a)-(d) the side chains rendered as sticks are those within 4 Å of an iron ion.

Figure 3.

Mechanistic schemes illustrating the diversity of iron mineralization in ferritins. **(a)** Mechanism exemplified by vertebrate H-chain ferritins in which oxidation of two Fe^{2+} ions at the ferroxidase center results in an unstable di- Fe^{3+} form, leading to transfer of Fe^{3+} species into the cavity. Radical formation at the conserved near-ferroxidase center Tyr residue has been reported but substitution of the Tyr does not significantly affect the overall rate of mineralization and so the importance of the Tyr residue is not clear. **(b)** Mechanism exemplified by *E. coli* FtnA and other prokaryotic Ftn proteins in which site C is redox active, contributing to the overall $\text{Fe}^{2+}:\text{O}_2$ stoichiometry. Oxidation of three Fe^{2+} ions is coupled to oxidation of the conserved near-ferroxidase center Tyr residue leading to radical formation. Fe^{3+} is unstable at the ferroxidase center but to a lesser extent than in H-chain ferritin. **(c)** Mechanism exemplified by diatom ferritin in which site C is not redox active and only becomes occupied as Fe^{3+} exits from the ferroxidase center. In both (b) and (c), the presence of site C stabilizes Fe^{3+} at the center and thus significantly limits the flux of iron through the ferroxidase center. **(d)** Mechanism exemplified by *E. coli* BFR in which the ferroxidase center functions as a true catalytic cofactor site. Oxidation of two Fe^{2+} ion at the ferroxidase center generates a stable di- Fe^{3+} form that undergoes redox cycling driven by sequential oxidation of Fe^{2+} in the cavity and reduction of O_2 at the center. Reduction of the oxidized ferroxidase center is facilitated by transient radical formation on the conserved Tyr residue. Fe^{2+} ions are represented by orange spheres, Fe^{3+} ions by red spheres, and vacant iron binding sites by open spheres.

Figures

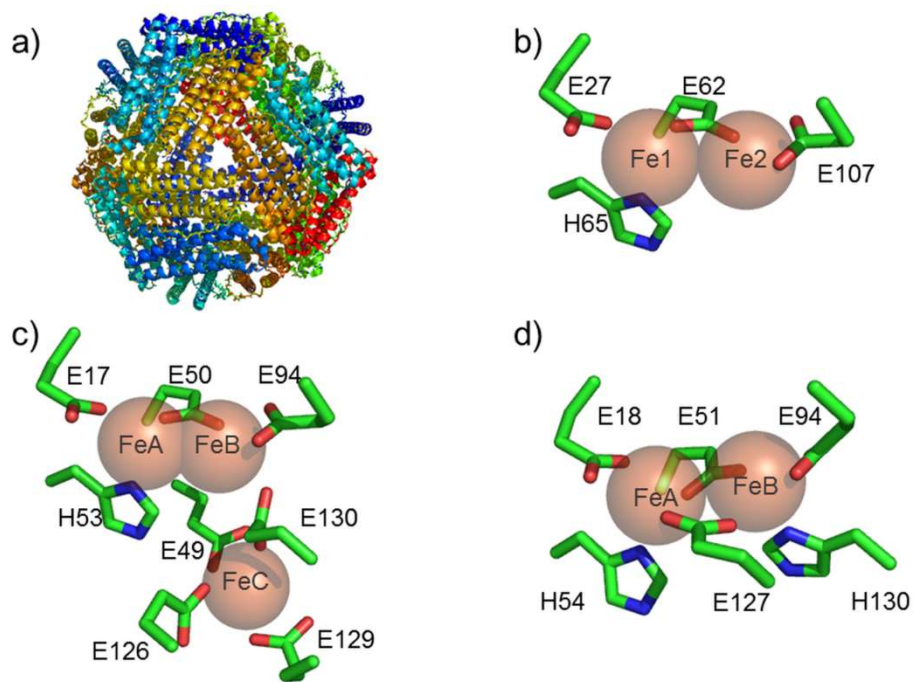


Figure 1

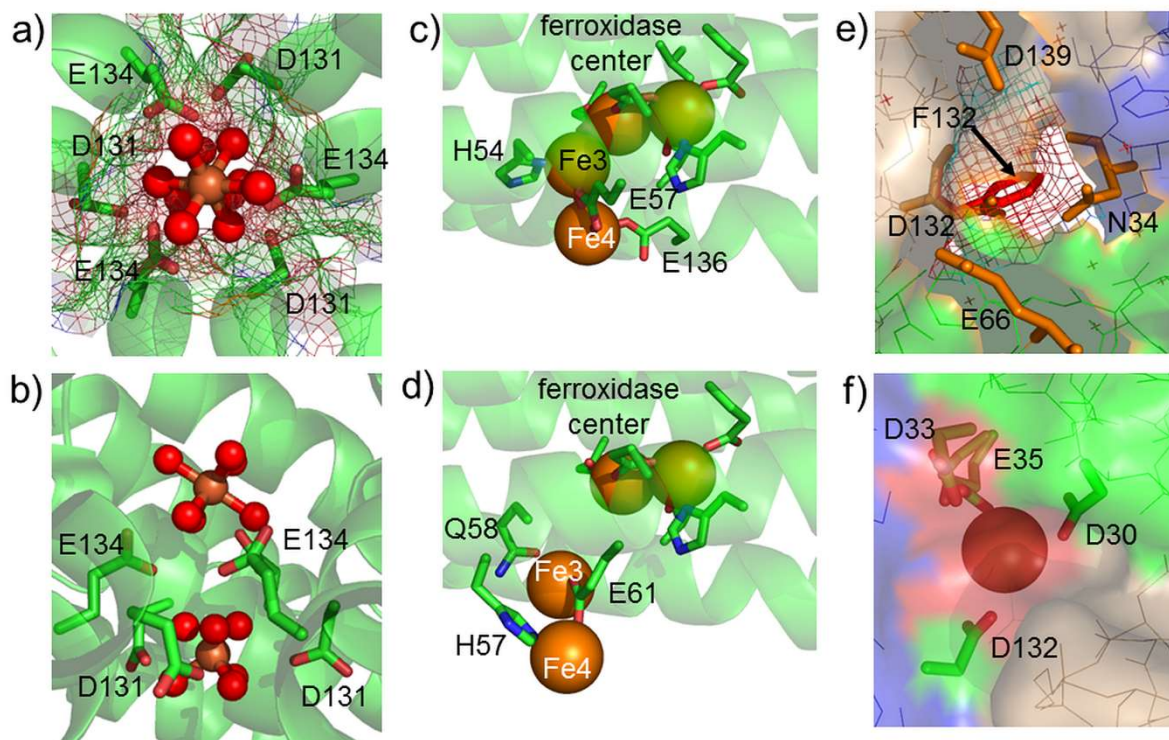


Figure 2

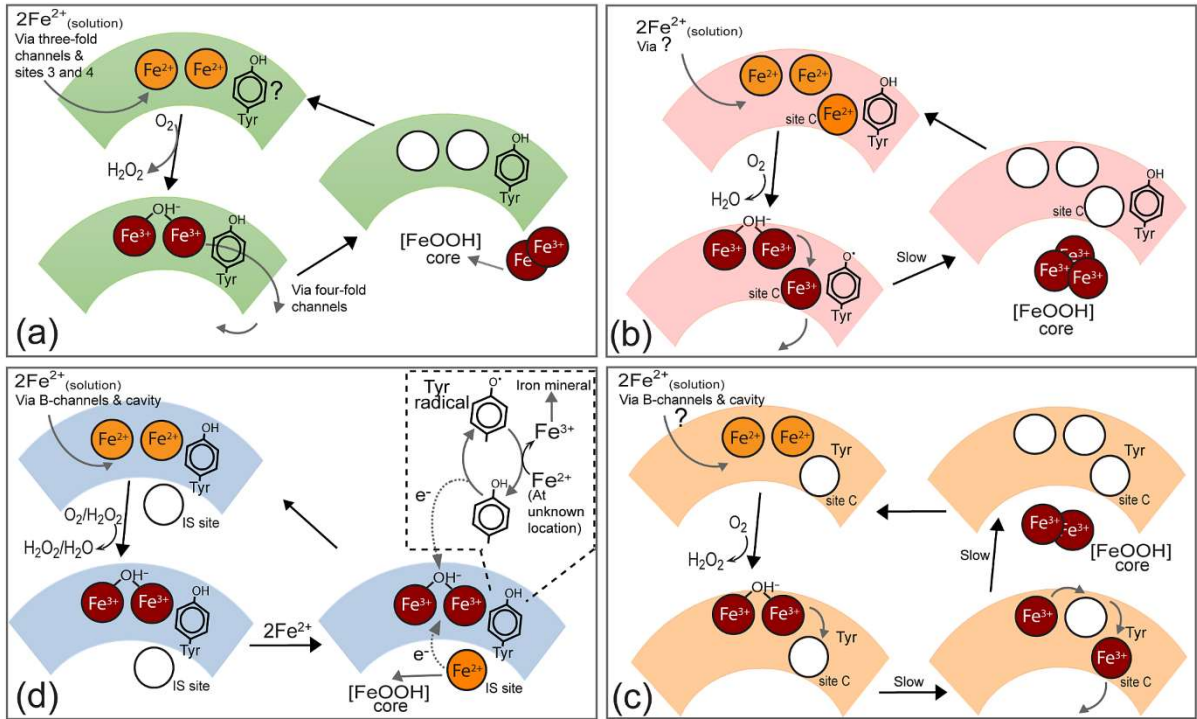


Figure 3